THE JOURNAL OF PHYSICAL CHEMISTRY B

ARTICLE

pubs.acs.org/JPCB

Glass Transition Dynamics of Room-Temperature Ionic Liquid 1-Methyl-3-trimethylsilylmethylimidazolium Tetrafluoroborate

Georgina Jarosz, Michal Mierzwa, Jerzy Zioło, and Marian Paluch*

Institute of Physics, University of Silesia, Uniwersytecka 4, 40-007 Katowice, Poland

Hideaki Shirota

Department of Nanomaterial Science & Department of Chemistry, Chiba University, 1-33 Yayoi, Inage-ku, Chiba 263-8522, Japan

K. L. Ngai

CNR-IPCF, Dipartimento di Fisica, Largo Bruno Pontecorvo 3, I-56127, Pisa, Italy

ABSTRACT: The conductivity relaxation dynamics of the room-temperature ionic liquid 1-methyl-3-trimethylsilylmethylimidazolium tetrafluoroborate ([Si-MIm][BF_4]) have been studied by broadband conductivity relaxation measurements at ambient pressure and elevated pressures up to 600 MPa. For the first time, several novel features of the dynamics have been found in a room-temperature ionic liquid. In the electric loss modulus $M''(f)$ spectra, a resolved secondary β-conductivity relaxation appears, and its relaxation time τ_β shifts on applying pressure in concert with the relaxation time τ_α of the primary α-conductivity relaxation. The spectral dispersion of the α-conductivity relaxation, as well as the fractional exponent $(1 - n)$ of the Kohlrausch−Williams−Watts function that fits the spectral dispersion, is invariant to various combinations of pressure and temperature that keep τ_α constant. Moreover, τ_β is unchanged. Thus the three quantities, τ_α, τ_β, and n, are coinvariant to changes in pressure and temperature. This strong connection to the α-conductivity relaxation shown by the β-conductivity relaxation in [Si-MIm][BF_4] indicates that it is the analogue of the Johari−Goldstein β-relaxation in nonionically conducting glass-formers. The findings have fundamental implications on theoretical interpretation of the conductivity relaxation processes and glass transition in ionic liquids. It is also the first time such a secondary conductivity relaxation or the primitive conductivity relaxation of the coupling model has been fully resolved and identified in $M''(f)$ in any ionically conducting material that we know of.

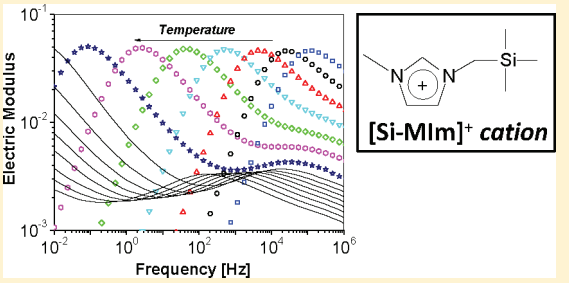

1. INTRODUCTION

Ionic liquids (ILs) of current interest in the physical chemistry and chemical physics research communities are composed mostly of an aromatic organic cation (occasionally organic nonaromatic cation) and a variety of inorganic and organic anions. Those ILs having melting temperature and glass transition temperature below room temperature are called room-temperature ionic liquids (RTILs). The studies of ILs are motivated principally by their many potential applications.[1−8] Moreover, the number of ILs that can be fabricated by many different combinations of known cations and anions offer a wealth of materials with diverse dynamics and transport properties in the class to be studied.

Aside from interest in applications, the study of ILs can benefit other research areas, such as glass transition and ionic conductivity relaxation since the ILs are glass-forming and ionically conducting. The fact that the physical properties of the ILs can be varied over large ranges by changing the chemical composition makes them ideal for the study of fundamental questions on dynamics of ionically conducting glass-forming liquids and in the glassy state. Studies in this direction at temperature encompassing the glass transition temperature, T_g, have been carried out by several groups using different methods. Here we mention examples from quasielastic neutron scattering,[9,10] mechanical relaxation,[11] dielectric relaxation,[12−17] light scattering,[12] adiabatic calorimetry,[18] and quasielastic Raman scattering.[19]

In all previous studies related to the dynamics of glass transition, the side chain of the aromatic central molecule of the cation is an alkyl chain of various lengths. In 2005, Shirota and Castner[20] synthesized a new class of silicon-substituted imidazolium cation, with the Si in a side group of an imidazolium cation. More exactly, the cation is 1-methyl-3-trimethylsilylmethylimidazolium, $[Si\text{-}MIm]^+$. The novel feature in the chemical structure is the trimethylsilylmethyl group instead of the alkyl chain. By replacing the trimethylsilylmethyl group in $[Si\text{-}MIm]^+$ with the analogous neopentyl group, they synthesized the closely

Received: July 30, 2011
Revised: September 25, 2011
Published: September 27, 2011

related cation, 1-methyl-3-neopentylimidazolium, $[C\text{-}MIm]^+$. ILs are made by either $[Si\text{-}MIm]^+$ or $[C\text{-}MIm]^+$ as the cation and tetrafluoroborate $[BF_4]^-$ or bis(trifluoromethylsulfonyl)-amide $[NTf_2]^-$ as the anion. The properties of the ILs are compared, which include the ultrafast intermolecular, vibrational, and orientational dynamics obtained by femtosecond Raman-induced Kerr effect spectroscopy (RIKES),[20] shear viscosity measurements, and self-diffusion coefficients from nuclear magnetic resonance.[21] All such data were collected at temperatures above 283 K, much higher than $T_g = 216$ K in the case of $[Si\text{-}MIm]^+$. Thus, nothing is known about the dynamics of $[Si\text{-}MIm]^+$ and $[C\text{-}MIm]^+$ at lower temperatures in the liquid state or in the glassy state. In view of the difference in the chemical structures of ILs based on $[Si\text{-}MIm]^+$ and $[C\text{-}MIm]^+$ as cations from all previous studies, we seize the opportunity of making broadband conductivity relaxation measurements of these ILs at ambient and elevated pressures. Reported in this paper are the results of the IL 1-methyl-3-trimethylsilylmethylimidazolium tetrafluoroborate, $[Si\text{-}MIm][BF_4]$, with $[Si\text{-}MIm]^+$ as the cation and $[BF_4]^-$ as the anion. As presented below, the conductivity relaxation dynamics of $[Si\text{-}MIm][BF_4]$ in both the equilibrium liquid state and the glassy state exhibit practically all the fundamental and universal properties of nonionically conducting glass-formers, not seen before in the previous studies of the more common ILs or other ionically conducting materials.

2. EXPERIMENTAL METHODS

Sample Preparation. The sample IL $[Si\text{-}MIm][BF_4]$ was synthesized according to the previous report.[20] Briefly, $[Si\text{-}MIm]$-Cl was synthesized as a precursor for $[Si\text{-}MIm][BF_4]$. 1-Methylimidazole was distilled before use. Trimethylsilylmethyl chloride was added to 1-methylimidazole at nitrogen atmosphere in a flask equipped with a reflux condenser and magnetic stirrer, and the solution was heated to approximately 80 °C in an oil bath for 8 h while stirring. Then the flask was allowed to cool to room temperature. The obtained oil was then washed by ethyl acetate five times. The residue and activated carbon were mixed with acetonitrile, and stirred at room temperature overnight. The solution was filtered and evaporated. The obtained IL was dried in vacuo at 313 K for more than 2 days. Then, the anion was exchanged. 1-Methyl-3-trimethylsilylmethylimidazolium chloride was dissolved in water. Sodium tetrafluoroborate was dissolved in water, and the aqueous solution was added to the aqueous imidazolium solution. After the mixture was stirred at room temperature for 1 h, the aqueous solution was decanted. The IL layer was dissolved in dichloromethane and washed with water six times. The dichloromethane was evaporated. The residue and activated carbon were mixed with acetonitrile, and stirred at room temperature overnight. The solution was filtered and evaporated. The obtained IL was dried in vacuo at 313 K for more than 2 days. ^{1}H-NMR (500 MHz, d_6-DMSO): 0.06 (s, 9H, $SiCH_3$), 3.83 (s, 3H, NCH_3), 3.87 (s, 2H, NCH_2), 7.57 (t, $J = 1.7$ Hz, 1H, $CH_3NCHCHN$), 7.67 (t, $J = 1.7$ Hz, 1H, $CH_3NCHCHN$), 8.90 (s, 1H, NCHN). MS (+ve): m/z 169 ($[Si\text{-}MIm]^+$), 425 ($[Si\text{-}MIm]_2[BF_4]^+$) ; MS (-ve): m/z 87 ($[BF_4]^-$), 343 ($[Si\text{-}MIm][BF_4]_2^-$). The water content of the IL was measured by Karl Fischer titration using a coulometer (Hiranuma, AQ-300) and was found to be 50.4 ppm.

Conductivity Relaxation Measurements. Isobaric dielectric measurements at ambient pressure were carried out using a Novo-Control GMBH Alpha dielectric spectrometer (10^{-2}—10^7 Hz). The sample was placed between two stainless steel flat electrodes of the capacitor with a gap of 0.1 mm. The temperature was controlled by the Novo-Control Quattro system, with use of a nitrogen-gas cryostat. The temperature stability of the samples was better than 0.1 K.

Measurements at high pressure (at Silesian University) employed a technique similar to that of Johari and Whalley.[22] The liquid sample and parallel plate capacitor were placed in a Teflon bellows mounted in the high pressure chamber. Pressure was measured by a Nova Swiss tensometric meter with an accuracy of 3 MPa. Temperature was controlled to within 0.2 K by means of liquid flow from a thermostatic bath. More details about high pressure dielectric measurements can be found in ref 23.

3. CONDUCTIVITY RELAXATION MEASUREMENTS AT AMBIENT PRESSURE

We present first the isothermal dielectric relaxation measurements of $[Si\text{-}MIm][BF_4]$ at ambient pressure as a function of frequency f over a range of temperatures T above and below $T_g = 211$ K. The quantities measured directly by experiment are the capacitance $C(f)$ and the conductance $G(f)$, from which the electrical conductivity response of the IL can be given equivalently in three forms: the complex conductivity, $\sigma^*(f)$, the complex permittivity, $\varepsilon^*(\omega)$, and the complex electric modulus $M^*(f)$. They are equivalent because of the identities, $M^*(f) \equiv 1/\varepsilon^*(f) \equiv i\omega\varepsilon_o/\sigma^*(f)$, where ε_o is the permittivity of a vacuum. Since $[Si\text{-}MIm][BF_4]$ is an ionic conductor, its electrical response is best represented by the complex electric modulus,[24] $M^*(f) = M'(f) + iM''(f)$. The dynamics of the structural relaxation can be inferred from the electrical conductivity relaxation in the temperature range where the two processes are coupled to each other. However, as shown before in the other IL (1-butyl-3-methylimidazolium hexafluorophosphate (abbreviated as BMIM-HFP[13] or BMIM-PF_6[12b]), in its supercooled state like in the present case and near the glass transition temperature, the conductivity relaxation decouples from the structural relaxation. Specifically, the temperature dependence of the electric modulus relaxation time becomes weaker than η/T when temperature falls below $1.1T_g$, where η is the viscosity. Hence BMIM-HFP (or BMIM-PF_6) shows the enhanced translational diffusion or fractional Stokes—Einstein behavior observed in some supercooled liquids.[12b,13,14] The viscosity of $[Si\text{-}MIm][BF_4]$ had been measured at temperatures higher than 280 K, way above T_g and the entire temperature range of the conductivity relaxation measurements presented in this paper. Thus, the question of whether the conductivity relaxation decouples from η/T or rotational relaxation in $[Si\text{-}MIm][BF_4]$ at temperatures near T_g cannot be answered until extensive viscosity measurements become available in the future. The orientational relaxation of the cation is suppressed while the conductivity is enhanced in the electric loss modulus representation of the measurements as done here. Hence our dielectric measurements cannot detect or resolve the orientational relaxation as well as similar measurements by others.[12,13,15,16] Another technique such as the time-resolved phosphorescence spectroscopy for solvation dynamics has to used to observe the rotation relaxation of the cation unobstructed by the conductivity relaxation, as demonstrated by Ito and Richert.[13,14]

Figure 1 shows the frequency dependence of the electric loss modulus, $M''(f)$, for $[Si\text{-}MIm][BF_4]$ at atmospheric pressure and different temperatures from 243 to 173 K, some above and some

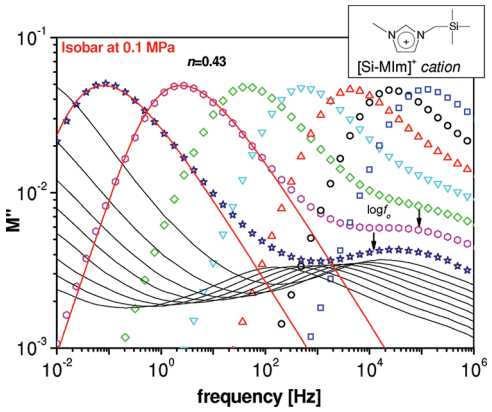

Figure 1. Imaginary part of the complex electric modulus, $M''(f)$, of [Si-MIm][BF_4] versus frequency at ambient pressure and constant temperature with temperature in the range 243−173 K, spanning across T_g. The spectra were measured at intervals of 5 K each. The data represented by symbols range from 243 to 213 K. Data from 208 to 173 K are not shown by symbols, otherwise they overlap and the features cannot be clearly discerned. To avoid this undesirable situation, the data are interpolated by black lines to show the shift of the secondary β-conductivity relaxation on decreasing temperature. The red lines are fits to the slower primary α-conductivity relaxation loss peak at two temperatures by the Fourier transform of the Kohlrausch−Williams−Watts (KWW) function. The secondary β-conductivity relaxation are resolved above and below T_g. The arrows indicate the locations of the logarithm of the primitive conductivity relaxation frequencies, log f_0, which are in agreement with the most probable β-conductivity relaxation frequencies within a factor of about 2.

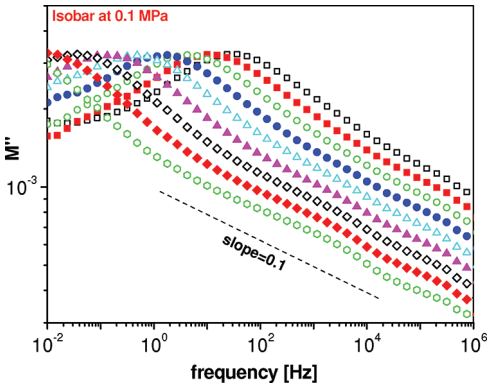

Figure 2. Imaginary part of the complex electric modulus, $M''(f)$, of [Si-MIm][BF_4] versus frequency at ambient pressure and constant temperature with temperature in the range 163−123 K, way below T_g. The spectra, measured every 5 K, show the presence of the slower well-resolved secondary β-conductivity relaxation and the NCL at higher frequencies.

below T_g. At several temperatures above T_g, the spectra show the presence of two loss peaks. If conductivity relaxation and structural relaxation are coupled together, the loss peak at lower frequency corresponds to the structural α-relaxation, and the one at higher frequency is the accompanying secondary relaxation commonly found in glass-formers of different kinds. However, in view of the possibility that the two relaxations are decoupled in the temperature range of our measurements, the slower and faster processes observed in Figure 1 are referred to as the primary α-conductivity relaxation and secondary β-conductivity relaxation, respectively. The α-conductivity relaxation appears as an asymmetric loss peak with width broader than the Debye peak in $M''(f)$, the maximum of which determines the most probable conductivity relaxation frequency. These features are typical of many ionic conductors, organic or inorganic, molten, crystalline, or glassy.[24−29] The frequency dependence of the complex electric modulus $M^*(f)$ comes from the time dependence of the correlation function $\Phi(t)$ of ion motion via the Fourier transform

$$M^*(\omega) = M' + iM'' = M_\infty[1 - \int_0^\infty dt \exp(-i\omega t)(-d\Phi/dt)] \quad (1)$$

Here M_∞ is the reciprocal of the high frequency dielectric constant ε_∞. In the absence of interaction and correlation between the ions, motions of ions are independent of each other. A linear exponential time dependence, $\exp(-t/\tau_0)$, for $\Phi(t)$ applies, and from eq 1 $M''(f)$ is a symmetric Debye loss peak with full-width at half-maximum equal to 1.144 decade. This is not the case for $M''(f)$ of [Si-MIm][BF_4] in Figure 1 at any temperature. Like in all ionic conductors that have high density of ions, ion−ion interaction and correlations are predominant, and the effects on conductivity relaxation are non-negligible. Following the tradition in analyzing the $M''(f)$ data of ionic conductors,[24−29] the asymmetric and broad α-loss peak of [Si-MIm][BF_4] in Figure 1 is fitted by $M''(f)$ calculated by using the Kohlrausch stretched exponential correlation function:

$$\Phi(t/\tau_\alpha) = \exp[-(t/\tau_\alpha)^{1-n}] \quad (2)$$

where τ_α is the α-conductivity relaxation time and the fractional quantity, $0 < n < 1$, in the exponent indicates the deviation from linear exponential time dependence for independent ion motion, or is a measure of the effect due to interaction and correlation. Shown in Figure 1 are the fits to $M''(f)$ at two temperatures with $n = 0.43$. The deviation of the data from the fit at higher frequencies is due to the contributions from faster processes including the resolved secondary β-conductivity relaxation, all part of the evolution of the many-body relaxation with time. The use of the two arrows and their label, log f_0, will be explained later after the spectra taken at elevated pressures have been presented.

The β-conductivity relaxation continues to be observed below T_g as shown in Figure 1 and also in Figure 2 further down in temperatures within the range $163 \le T \le 123$ K, deep into the glassy state. Spectra at lower temperatures in Figure 2 show that the β-loss peak gives way at higher frequencies to $M''(f)$ assuming approximately the power law dependence of $M''(f) \propto (f)^{-0.1}$. This feature at higher frequencies of the loss, appropriately called the nearly constant loss (NCL) because of the small exponent in the power law, is commonly observed in many glass-formers[30−34] and ionic conductors[35,36] of different types. The equivalent of the NCL was found in the study of the orientational dynamics of the supercooled IL *N*-propyl-3-methylpyridinium bis(trifluoromethylsulfonyl)imide (PMPIm), by optically heterodyne-detected optical Kerr effect experiments in the picoseconds to nanoseconds time range, corresponding to the intermediate power law, pt^{-z} with $z \approx 1$, in the Kerr effect data.[37] It is gratifying in the present work to find NCL in $M''(f) \propto (f)^{-0.1}$ from conductivity relaxation in [Si-MIm][BF_4], at lower temperatures in the glassy state, and at much longer times corresponding to the dielectric frequency range of $1 < f < 10^6$ Hz. If plotted as log $\sigma(f)$ versus log f, the present data show at

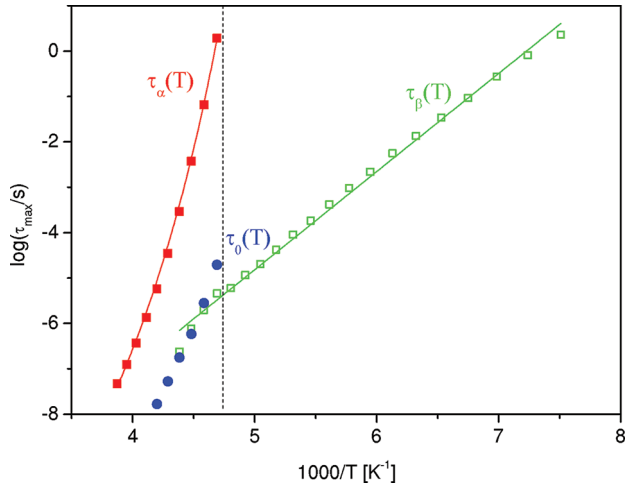

Figure 3. Temperature dependences of the α- and β-conductivity relaxation times obtained at ambient pressure. Predictions for the JG relaxation times above T_g according to CM are plotted as the solid blue circles. The solid lines are fits to the VFTH equation, $\log \tau_\alpha = -16.67 + 920/(T - 159\ \mathrm{K})$, and the Arrhenius law with $E_A = 41$ kJ/mol.

high frequencies that $\sigma(f)$ has the frequency dependence of f^{1-c} with $c \sim 0.1$, similar to that found by others in BMIM-PF_6.[12b] This same NCL phenomenon seen in the RTILs is found in many inorganic ionic conductors (glassy,[35,36] crystalline,[30] or molten[25]) where the ions are charged particles such as alkali ions, suggesting a common origin. For ionic conductors where the ions are charged atoms, NCL is a commonly used term to describe loss, $M''(f) \propto (f)^{-c}$ or $\sigma(f) \propto (f)^{1-c}$, with c being small. References to papers of various workers using this term can be found in a review.[24] In nonionically conducting glass-formers, dielectric loss from molecular rotation also shows similar behavior with $\varepsilon''(f) \propto (f)^{-c}$. We used the same term NCL and the same interpretation of its origin for both ionically conducting materials and nonionically conducting glass-formers with experimental support.[30,32−34] Notwithstanding, it is worthwhile to mention a different terminology for the same property in nonionically conducting glass-forming liquids used by Rössler and co-workers.[38,39] They consider the $\varepsilon''(f) \propto (f)^{-c}$ as a special case of the "excess wing" appearing on the high frequency flank of the α-loss peak. In the present case of [Si-MIm][BF_4], the "excess wing" in $M''(f)$ is not on the high frequency flank of the α-conductivity relaxation, but rather the β-conductivity relaxation.

The NCL has been interpreted as loss due to motion of ions or molecules within cages defined by anharmonic intermolecular potential at times before the commencement of a specific secondary relaxation causing decay of the cages.[30−36] Plenty of experimental evidence supporting this can be found in refs 30, 33, 35, and 36. To be effective in causing cage decay, the specific secondary relaxation involves the rotation and/or translation of the entire molecule.[40] This specific secondary relaxation has been referred to as the Johari−Goldstein (JG) β-relaxation to distinguish it from other secondary relaxations that involve motion of only part of the molecule. Many properties of the JG β-relaxation are so distinctive that criteria have been established to identify it.[41] Apart from the role that JG β-relaxation plays in cage decay resulting in terminating the NCL regime, it is also the precursor of the structural α-relaxation. Various connections or relations between the JG β-relaxation and the α-relaxation found experimentally have shown the fundamental importance of the JG β-relaxation.[42] Examples included the pressure dependence of both relaxations,[43−45] which is also found in [Si-MIm][BF_4], and to be discussed in the following section.

The relaxation times τ_α and τ_β of the α- and β-conductivity relaxations, respectively, in [Si-MIm][BF_4] have been determined as a function of temperature by either fitting the spectra or effectively by reading off the α- and β-loss peak frequencies. This is because both the α- and β-loss peaks are well resolved, and the difference in the results obtained by the two procedures is negligible. The results are plotted against reciprocal temperature in Figure 3, where the glass transition temperature T_g is indicated. The temperature dependence of τ_α is like that of the Vogel−Fulcher−Tammann−Hesse (VFTH) form, $\log \tau_\alpha = \log \tau_0 + A/(T - T_0)$, typical of α-relaxation in glass-formers. While the temperature dependence of τ_β is Arrhenius, $\tau_\beta = \tau_\infty \exp(E_A/RT)$, below T_g in the glassy state, it changes after crossing some temperature near T_g to assume a stronger T-dependence in the liquid state. This behavior is commonly found in the τ_β of JG β-relaxation of many nonionically conducting glass-formers.[41−43] It is an example of the connection in properties between the α- and β-conductivity relaxations because τ_α also changes its temperature dependence in the same manner when crossing T_g. The identity of the data represented by closed circles and the label, τ_0, for them will be given later in the Discussion section.

4. CONDUCTIVITY RELAXATION MEASUREMENTS AT ELEVATED PRESSURES

Study of the dynamics at elevated pressures P is beneficial for a deeper understanding of the nature of the α- and β-conductivity relaxations as proven in previous reports on works performed mostly for nonionically conducting glassformers.[42−48] Two seemingly general and spectacular properties in non-hydrogen-bonded and nonionically conducting glass-formers observed experimentally at different combinations of P and T while keeping τ_α constant are (1) the frequency dispersion of the α-relaxation is unchanged (i.e., temperature−pressure superpositioning), and (2) τ_β of the JG β-relaxation also remains unchanged. Unchanged frequency dispersion implies that the fractional exponent, $(1 - n)$, of the stretched exponential function in eq 1 used to fit the α-dispersion is also unchanged. Thus, the two observed properties can be combined into one statement as the coinvariance of the three quantities, τ_α, n, and τ_β, to different combinations of P and T.

For ILs, so far only one study of 1-butyl-1-methylpyrrolidinium bis[oxalate]-borate (BMP-BOB) at elevated pressures has been reported.[15] The spectral dispersion of the α-conductivity relaxation broadens with increasing τ_α, but was found to be the same on varying the combinations of P and T while keeping τ_α constant. Hence temperature−pressure superpositioning of the α-conductivity relaxation is obeyed. A secondary conductivity relaxation process was resolved in the loss modulus spectra in another IL, BMP-BOB.[15] However, its relaxation time is practically independent of pressure, which indicates that it is not the JG β-conductivity relaxation of BMP-BOB. Apparently the JG β-conductivity relaxation in BMP-BOB is not resolved. Present in the $M''(f)$ of BMP-BOB is a broad wing on the high frequency flank of the α-loss peak in excess of the fit by the stretched exponential function in eq 1. This wing is likely due to the unresolved JG β-conductivity relaxation because it also obeys

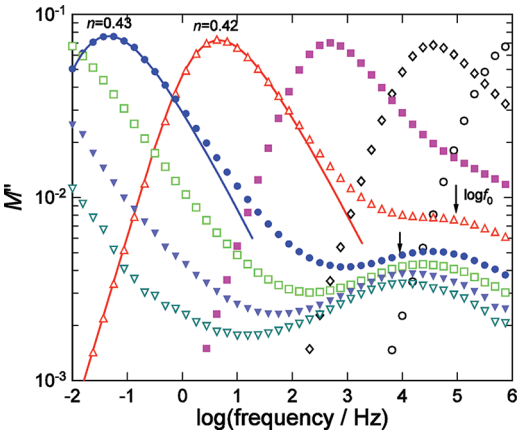

Figure 4. Imaginary part of the complex electric modulus, $M''(f)$, of [Si-MIm][BF_4] versus frequency at fixed T = 253 K and varyiable pressure, starting at the ambient pressure of 0.1 MPa on the far right (open circles) and at elevated pressures from 100 (open diamonds) to 600 MPa (closed inverted triangles) in increments of 100 MPa each in going from right to left. The open inverted triangles are the data at 600 MPa and T = 253 K after aging the sample for 12 h while keeping pressure temperature constant. The arrows indicate the locations of the logarithm of the primitive conductivity relaxation frequencies, log f_0, which are in agreement with the most probable β-conductivity relaxation frequencies within a factor of about 2.

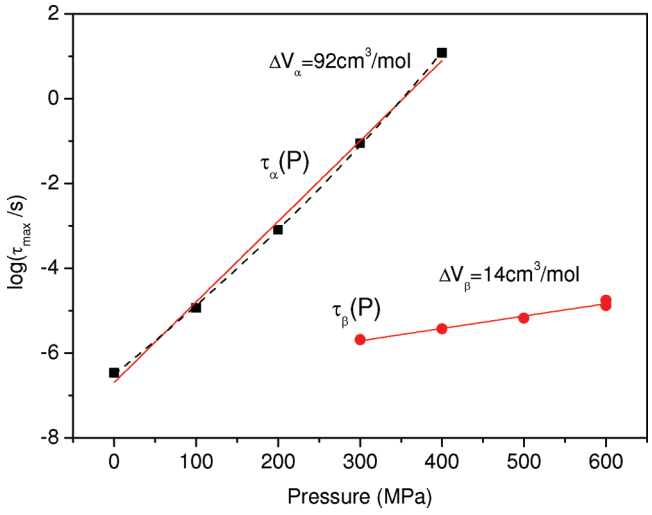

Figure 5. Pressure dependences of the α- and β-conductivity relaxation times at T = 253 K. The solid lines are fits to the simple volume activated law, eq 3. The dashed curve represents the fit to the pressure counterpart of the VFTH equation for temperature variation with the following values of parameters: log τ_0 = −6.5, D = 76, and P_0 = 2.1 GPa.

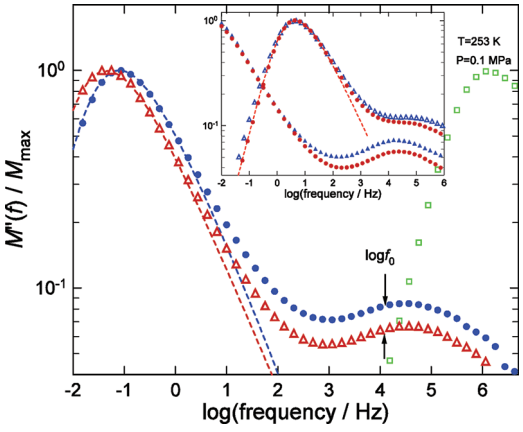

Figure 6. Normalized $M''(f)$ spectra at different combinations of P and T to show coinvariance of τ_α, τ_β, and n at constant τ_α. Red open triangles: P = 600 MPa, T = 253 K. Blue circles: P = 0.1 MPa, T = 213 K. Green open squares: P = 0.1 MPa, T = 253 K. Blue and red lines are fits by Fourier transform of the stretched exponential correlation function given by eq 2 with n = 0.43. The inset shows coinvariance at two more constant values of τ_α. Blue triangles are data at ambient pressure and T = 218 and 208 K from right to left. Red filled circles are data at constant T = 253 K and P = 300 and 500 MPa from right to left. There is not a perfect match of the peak frequency of data taken at T = 218 K and P = 0.1 MPa with that taken at T = 253 K and P = 300 MPa. The comparison is made by shifting the ambient pressure data to higher frequencies by a factor of 1.5. Note that the width of the α-conductivity relaxation loss peak increases slightly on increasing τ_α toward glass transition. The arrows indicate the locations of the logarithm of the primitive conductivity relaxation frequencies, log f_0, which are in agreement with the most probable β-conductivity relaxation frequencies within a factor of about 2.

time-pressure superpositioning. Notwithstanding, this is not convincing evidence of the existence of the JG β-relaxation and coinvariance of τ_α, n, and τ_β in ILs. An earlier dielectric study of another IL, BMIM-BMSF,[12] at ambient pressure found two secondary relaxations, with the slower secondary relaxation proposed as the JG β-conductivity relaxation. The authors of ref 12 made this conclusion based on its relaxation time having an activation energy $E_a = 24RT_g$ obeyed by JG β-relaxation in some nonionically conducting glass-formers. However, this criterion for JG β-relaxation is loose because it has been shown that non-JG β-relaxation in some glass-formers also obeys the relation $E_a = 24RT_g$, and there is a large spread in the ratio of E_a/RT_g for genuine JG β-relaxations.[49] The critical test was made by applying pressure to BMIM-BMSF, and it was found that the purported JG β-relaxation does not shift in frequency on elevating pressure, and thus again the true JG β-relaxation of BMIM-BMSF was not resolved.

To investigate whether the secondary conductivity relaxation of [Si-MIm][BF_4] resolved in the isothermal $M''(f)$ spectra at ambient pressure (Figures 1 and 2) is the JG β-conductivity relaxation or not, we performed dielectric measurements on the same sample at fixed T = 253 K and varying pressure, starting at the ambient pressure of 0.1 MPa and increasing up to 600 MPa. The measured $M''(f)$ are presented in Figure 4. By inspection of the figure, it is evident that both the α- and the β-conductivity relaxations shift to lower frequencies on increasing pressure. The sensitivity of τ_β to pressure is one strong indication that the resolved secondary conductivity relaxation is the JG β-conductivity relaxation in [Si-MIm][BF_4] that has eluded detection in ILs so far. The spectrum taken at 600 MPa (closed inverted triangles) is in the glassy state. On aging the sample after 12 h while keeping pressure at 600 MPa and T = 253 K, the entire data (filled inverted triangles) shifts to lower frequencies (open inverted triangles). The shifts are not uniform: the higher the frequency, the less the shift. The sensitivity of the β-conductivity relaxation to aging is another indication that it is well connected to the α-relaxation.

The pressure dependences of τ_α and τ_β at T = 253 K determined from the spectra in Figure 4 are brought out individually in Figure 5. For the limited data gathered, the pressure

dx.doi.org/10.1021/jp207291k | J. Phys. Chem. B 2011, 115, 12709–12716

dependence of the relaxation times were analyzed in terms of the simple volume activated equation,[50]

$$\tau(P,T) = \tau_v(0,T)\exp\left(\frac{P\Delta V}{RT}\right) \quad (3)$$

By fitting the pressure dependences of the relaxation times, we obtained the values of activation volume $\Delta V_\alpha = 92$ cm^3/mol and $\Delta V_\beta = 14$ cm^3/mol for τ_α and τ_β, respectively. However, in the case of the pressure dependence of the α-conductivity relaxation times, we found that the pressure counterpart of the VFTH equation for temperature variation[51] provides a better fit to the experimental data.

$$\tau(P) = \tau_0\exp\left(\frac{D_P P}{P_0 - P}\right) \quad (4)$$

The fit is shown in Figure 5, and the parameters used are given in the figure caption.

The $M''(f)$ loss peak at ambient pressure in Figure 1 and that at elevated pressure in Figure 4 do not have exactly the same height. For comparison of the frequency dispersion of the α-relaxation at $P = 0.1$ MPa and $T = 213$ K with that at $P = 600$ MPa and $T = 253$ K, we normalize both spectra by the maximum loss, and the normalized spectra are shown in Figure 6. There is a small difference in the frequencies of the loss maxima in the two spectra, and hence the relaxation times τ_α are not exactly the same. Ignoring this small difference in τ_α, it can be seen from the data and the fits by the KWW function with the same exponent, $(1 - n)$, in Figure 6 that the frequency dispersion of the α-conductivity relaxation is the same for these two combinations of P and T. Both are well fitted by the Fourier transform of the stretched exponential correlation function with the same $n = 0.43$. Furthermore, the resolved secondary relaxation remains at the same location, and hence τ_β is practically unchanged. Hence, the properties observed can be summarily stated as coinvariance of the three characteristic quantities, τ_α, τ_β, and n, to changes in pressure and temperature. Also shown in Figure 6 is the α-loss peak at ambient pressure of 0.1 MPa and $T = 253$ K. There is a shift of more than 7 decades of τ_α on elevating ambient pressure to 600 MPa at $T = 253$ K. Since the JG β-conductivity relaxation is located at higher frequencies than the α-loss peak at $P = 0.1$ MPa and $T = 253$ K, we can infer that there is a shift of more than 2.5 decades of τ_β on elevating pressure from 0.1 to 600 MPa. This estimate demonstrates the high sensitivity of τ_β to pressure. The inset in Figure 6 shows that the coinvariance of τ_α, τ_β, and n holds in two other situations with different values of these parameters, and thus the coinvariance is general.

Taking all the above together, we have found coinvariance of τ_α, n, and τ_β for conductivity relaxation in an IL, namely [Si-MIm]-[BF_4], for the first time. This property proves beyond any doubt that the resolved secondary conductivity relaxation of [Si-MIm]-[BF_4] is the JG β-conductivity relaxation. For both ionically conducting and nonionically conducting glass-formers, the coinvariance has profound implications on the theory of the dynamics leading to glass transition. It indicates the fundamental role played by n and τ_β, and not just τ_α. Since the breadth of the α-relaxation measured by n increases with intermolecular interaction and constraints, from the participation of n in the coinvariance, we can infer the importance of many-body relaxation in determining τ_α besides thermodynamic factors such as volume and entropy. The involvement of τ_β in the coinvariance implies that it is inseparable from τ_α in theoretical treatment of the dynamics. From this we can infer that the dynamics is a continuously evolving relaxation processes with time. It effectively starts from the simple JG β-conductivity relaxation at times on the order of τ_β. As time increases, more ions participate in the processes. Finally, at times on the order of τ_α, it terminates with the α-conductivity relaxation having the maximum number of ions participating, which is determined by the nature and strength of the intermolecular interaction.

5. DISCUSSION AND CONCLUSION

Appearing in Figures 1, 4, and 6 is the frequency, f_0, the meaning of which has not been explained before. This is the primitive conductivity relaxation frequency related to the primitive conductivity relaxation time τ_0 of the coupling model (CM)[42,43,49,50] by the identity $\tau_0 = 1/2\pi f_0$. The similarity in properties between the primitive conductivity relaxation and the JG β-conductivity relaxation leads to the approximate equality of the two relaxation times, $\tau_0 \approx \tau_\beta$.[27,28,30,35,36,42] The principal prediction of the CM is the relation between τ_α and τ_0 involving n and given by

$$\tau_\alpha = [(t_c)^{-n}\tau_0]^{1/(1-n)} \quad (5)$$

Here, t_c is the crossover time from primitive conductivity relaxation with exponential time dependence to stretched exponential time dependence. Quasielastic scattering experiments on several ionic conductors, and small molecular and polymeric glass-formers have determined t_c to be about 1 to 2 ps.[41,42] The crossover at $t_c \approx 2$ ps was found by quasielastic neutron scattering measurements[9] on an RTIL, 1-*n*-butyl-3-methylimidazolium hexafluorophosphate, [bmim][PF_6], as can be seen by inspection of Figure 4 in ref 9. Some femtosecond optical heterodyne-detected RIKES experiments also observed in several RTILs at ambient conditions that the fastest relaxation process with time constant of approximately 2−3 ps is almost independent of the composition of the IL.[52−55] In the optically heterodyne-detected optical Kerr effect experiment on the supercooled IL PMPIm, discussed before in ref 37, a change of time dependence of the data near 2 ps occurs from a rapid decay, modeled by the power law at^{-s} with s as large as 4.3 at the shortest times, to the intermediate power law, pt^{-z} with $z \approx 1$. All the neutron and optical experiments mentioned above collectively show some fundamental changes of dynamics are occurring at times on the order of 2 ps in the ILs and also in other ionically conducting and nonionically conducting glass-formers.

We have calculated τ_0 from the τ_α and n obtained from the fits by eqs 1 and 2 to some of the spectra in Figures 1, 4, and 6. The location of the arrows indicated the calculated τ_0 expressed in terms of log f_0. The approximate agreement between f_0 and the peak frequency f_β of the resolved JG β-relaxation verifies the relation, $\tau_0 \approx \tau_\beta$, as shown collectively in Figure 3 for conductivity relaxation in the IL. The same relation was found before in many nonionically conducting glass-formers.[41,42] On replacing τ_0 with τ_β in eq 5, we arrive at the approximate relation

$$\tau_\alpha \approx [(t_c)^{-n}\tau_\beta]^{1/(1-n)} \quad (6)$$

This relation between τ_α, n, and τ_β immediately leads to coinvariance of the three quantities considering the fact that t_c is a constant, as found by experiment here in [Si-MIm][BF_4] and in many other glass-formers.

From the experimental data at ambient and elevated pressures presented above, there is ample evidence that all the basic and universal characteristics of the dynamics of nonionically conducting glass-formers are present in the conductivity relaxation of [Si-MIm][BF_4]. Found in this IL are the following items all for the first time in ILs: (1) The NCL, appearing at high frequencies/short times when molecules are caged, is terminated by the onset of the JG β-conductivity relaxation. (2) The JG β-relaxation is not only resolved, but its relaxation time is also highly pressure sensitive. (3) The invariance of the frequency dispersion of the α-relaxation (or the fractional exponent of the stretched exponential correlation function in eq 2) to different combinations of P and T at constant τ_α is found together with invariance of the ratio τ_α/τ_β. (4) There is approximate agreement between the experimentally observed τ_β and the primitive relaxation time τ_0 calculated by the CM relation. All the above properties of the conductivity relaxation dynamics found in the IL belong to the structural relaxation dynamics of many nonionically conducting glass-formers. Before closing, we mention two more such properties found by others. One is the temperature dependence of the elastic fixed energy scan by neutron scattering, which probes the fast processes when all molecules are caged, and is the counterpart of the NCL observed in the susceptibility spectrum. The elastic intensity from two neutron scattering experiments on [bmim][PF_6][9] and bmimCl[10] shows a change from a weaker temperature dependence to a stronger one on crossing T_g from below to above, exactly as found in conventional ionic conductors,[31,56] and in many nonionically conducting glass-formers.[30] Another is the superpositioning of dynamic properties such as viscosity, relaxation times, or diffusion coefficients under different conditions of temperature T, pressure P, and volume V by the scaling variable TV^γ (where γ is a material constant) observed experimentally as a general feature of many kinds of glass-forming materials.[23,57] The same TV^γ scaling was found in various ILs[58−60] as well as in 1-ethyl-3-methylimidazolium nitrate (EMIM-NO_3) by molecular dynamics simulation.[61] Thus, these general properties are common also to ILs, and their implications on theoretical interpretation of the overall conductivity relaxation dynamics of ILs cannot be ignored. Last but not least, it is first time that a genuine JG β-conductivity relaxation has been resolved and identified not only in ILs but also in any ionic conductor, glassy, crystalline, or molten.

AUTHOR INFORMATION

Corresponding Author

*E-mail: marian.paluch@us.edu.pl.

ACKNOWLEDGMENT

The support of the Polish State of Committee for Scientific Research (Grant No. N N202 023440) is gratefully acknowledged. This work was supported by the Ministry of Education, Culture, Sports, Science, and Technology (MEXT) of Japan (Grant-in-Aids for Young Scientists (A): 21685001 (H.S.)).

REFERENCES

(1) Wasserscheid, P., Welton, T., Eds. *Ionic Liquids in Synthesis*, 2nd ed.; Wiley-VCH: Weinheim Germany, 2008; ISBN 978-3-527-31239-9.

(2) Ohno, H., Ed. *Electrochemical Aspects of Ionic Liquids*; Wiley-Interscience: Hoboken, NJ, 2005; ISBN 978-0-471-64851-2.

(3) Seespecial issue on ionic liquids: *J. Phys. Chem. B* **2007**, *111*, 4639–5029.

(4) Chen, J. X.; Wu, H. Y.; Jin, C.; Zhang, X. X.; Xie, Y. Y.; Su, W. K. *Green Chem.* **2006**, *8*, 330.

(5) Migowski, P.; Machado, G.; Texeira, S. R.; Alves, M. C. M.; Morais, J.; Traverse, A.; Dupont, J. *Phys. Chem. Chem. Phys.* **2007**, *9*, 4814.

(6) Wojnarowska, Z.; Paluch, M.; Grzybowski, A.; Adrjanowicz, K.; Grzybowska, K.; Kaminski, K.; Wlodarczyk, P.; Pionteck, J. *J. Chem. Phys.* **2009**, *131*, 104505.

(7) Castner, E. W.; Wishart, J. F. J. *Chem. Phys.* **2010**, *132*, 120901.

(8) Shirota, H.; Fukazawa, H. Atom Substitution Effects in Ionic Liquids: A Microscopic View by Femtosecond Raman-Induced Kerr Effect Spectroscopy. In *Ionic Liquids: Theory, Properties, New Approaches*; Kokorin, A., Ed.; InTech: Rijeka, Croatia, 2011; pp 201−224.

(9) Triolo, A.; Russina, O.; Hardacre, C.; Nieuwenhuyzen, M.; Gonzalez, M. A.; Grimm, H. *J. Phys. Chem. B* **2005**, *109*, 22061.

(10) Inamura, Y.; Yamamuro, O.; Hayashi, S.; Hamaguchi, H. *Phys. B* **2006**, *385*, 732.

(11) Russina, O.; Beiner, M.; Pappas, C.; Russina, M.; Arrighi, V.; Unruh, T.; Mullan, C. L.; Hardacre, C.; Triolo, A. *J. Phys. Chem. B* **2009**, *113*, 8469.

(12) (a) Rivera, A.; Rössler, E. A. *Phys. Rev. B* **2006**, *73*, 212201. (b) Rivera, A.; Brodin, A.; Pugachev, A.; Rössler, E. A.; et al. *J. Chem. Phys.* **2007**, *126*, 114503.

(13) Ito, N.; Richert, R. J. *J. Phys. Chem. B* **2007**, *111*, 5016.

(14) Ngai, K. L. *J. Phys. Chem. B* **2006**, *110*, 26211.

(15) Rivera-Calzada, A.; Kaminski, K.; Leon, C.; Paluch, M. *J. Phys. Chem. B* **2008**, *112*, 3110.

(16) Sangoro, J.; Iacob, C.; Serghei, A.; Naumov, S.; Galvosas, P.; Kärger, J.; Wespe, C.; Bordusa, F.; Stoppa, A.; Hunger, J.; Buchner, R.; Kremer, F. *J. Chem. Phys.* **2008**, *128*, 214509.

(17) Weingartner, H.; Sasisanker, P.; Daguenet, C.; Dyson, P. J.; Krossing, I.; Slattery, J. M.; Schubert, T. *J. Phys. Chem. B* **2007**, *111*, 4775–4780.

(18) Yamamuro, O.; Minamimoto, Y.; Inamura, Y.; Hayashi, S.; Hamaguchi, H. *Chem. Phys. Lett.* **2006**, *423*, 371.

(19) Ribeiro, M. C. C. *J. Phys. Chem. B* **2007**, *111*, 5008.

(20) Shirota, H.; Castner, E. W., Jr. *J. Phys. Chem. B* **2005**, *109*, 21576.

(21) Chung, S. H.; Lopato, R.; Greenbaum, S. G.; Shirota, H.; Castner, E. W.; Wishart, J. F. *J. Phys. Chem. B* **2007**, *111*, 4885.

(22) Jorari, G. P.; Whalley, E. *Faraday Symp. Chem. Soc.* **1972**, *6*, 23.

(23) Roland, C. M.; Hensel-Bielowka, S.; Paluch, M.; Casalini, R. *Rep. Prog. Phys.* **2005**, *68*, 1405.

(24) Hodge, I. M.; Ngai, K .L.; Moynihan, C. T. *J. Non-Cryst. Solids* **2005**, *351*, 104.

(25) Howell, F. S.; Bose, R. A.; Macedo, P. B.; Moynihan, C. T. *J. Phys. Chem.* **1974**, *78*, 639.

(26) Richert, R.; Wagner, H. *Solid State Ionics* **1998**, *105*, 167.

(27) Ngai, K. L.; León, C. *Phys. Rev. B* **1999**, *60*, 9396.

(28) Ngai, K. L.; Rendell, R. W. *Phys. Rev. B* **2000**, *61*, 9393.

(29) Moynihan, C. T.; Boesch, L. P. *J. Non-Cryst. Solids* **1975**, *17*, 44.

(30) Ngai, K. L. *J. Phys.: Condens. Matter* **2003**, *15*, S1107.

(31) Casalini, R.; Ngai, K. L. *J. Non-Cryst. Solids* **2001**, *293−295*, 318.

(32) Sokolov, A. P.; Kisliuk, A.; Novikov, V. N.; Ngai, K. L. *Phys. Rev. B: Condens. Matter Mater. Phys.* **2001**, *63*, 172204.

(33) Capaccioli, S.; Shahin Thayyil, S. M. M.; Ngai, K. L. *J. Phys. Chem. B* **2008**, *112*, 16035.

(34) Ngai, K. L.; Paluch, M. *J. Phys. Chem. B* **2003**, *107*, 6865.

(35) Ngai, K. L.; Habasaki, J.; Hiwatari, Y.; León, C. *J. Phys.: Condens. Matter* **2003**, *15*, S1607.

(36) León, C.; Rivera, A.; Várez, A.; Sanz, J.; Santamaria, J.; Ngai, K. L. *Phys. Rev. Lett.* **2001**, *86*, 1279.

(37) Li, J.; Wang, I.; Fruchey, K.; Fayer, M. D. *J. Phys. Chem. A* **2006**, *110*, 10384.

(38) Brodin, A.; Rössler, E. A. *J. Chem. Phys.* **2006**, *125*, 114502.

(39) Brodin, A.; Rössler, E. A. *J. Chem. Phys.* **2007**, *126*, 244508.
(40) Ngai, K. L. *Philos. Mag.* **2004**, *84*, 1341.
(41) Ngai, K. L.; Paluch, M. *J. Chem. Phys.* **2004**, *120*, 857.
(42) Ngai, K. L. *Relaxation and Diffusion in Complex Systems*; Springer: New York, 2011.
(43) Mierzwa, M.; Pawlus, S.; Paluch, M.; Kaminska, E.; Ngai, K. L. *J. Chem. Phys.* **2008**, *128*, 044512.
(44) Kessairi, K.; Capaccioli, S.; Prevosto, D.; Lucchesi, M.; Sharifi, S.; Rolla, P. A. *J. Phys. Chem. B* **2008**, *112*, 4470.
(45) Bedrov, D.; Smith, G. D. *J. Non-Cryst. Solids* **2011**, *357*, 258.
(46) Hensel-Bielowka, S.; Paluch, M. *Phys. Rev. Lett.* **2002**, *66*, 25704.
(47) Casalini, R.; Roland, C. M. *Phys. Rev. Lett.* **2004**, *92*, 245702.
(48) Capaccioli, S.; Prevosto, D.; Lucchesi, M.; Rolla, P. A.; Casalini, R.; Ngai, K. L. *J. Non-Cryst. Solids* **2005**, *351*, 2643.
(49) Ngai, K. L.; Capaccioli, S. *Phys. Rev. E* **2004**, *69*, 031501.
(50) Floudas, G.; Paluch, M.; Grzybowski, A.; Ngai, K. L. *Molecular Dynamics of Glass-Forming Systems*; Springer-Verlag: Berlin, 2010.
(51) Paluch, M.; Rzoska, S. J.; Habdas, P.; Ziolo, J. *J. Phys.: Condens. Matter* **1996**, *8*, 10885.
(52) Fukazawa, H.; Ishida, T.; Shirota, H. *J. Phys. Chem. B* **2011**, *115*, 4621.
(53) Shirota, H.; Fukazawa, H.; Fujisawa, T.; Wishart, J. F. *J. Phys. Chem. B* **2010**, *114*, 9400.
(54) Shirota, H.; Funston, A. M.; Wishart, J. F.; Castner, E. W., Jr. *J. Chem. Phys.* **2005**, *122*, 184512.
(55) Giraud, G.; Gordon, C. M.; Dunkin, I. R.; Wynne, K. *J. Chem. Phys.* **2003**, *119*, 464.
(56) Ngai, K. L. *J. Chem. Phys.* **1999**, *110*, 10576.
(57) Casalini, R.; Roland, C. M. *Phys. Rev. E* **2004**, *69*, 062501.
(58) Paluch, M.; Haracz, S.; Grzybowski, A.; Pionteck, J.; Rivera-Calzada, A.; Leon, C. *J. Phys. Chem. Lett.* **2010**, *1*, 987.
(59) Roland, C. M.; Bair, S.; Casalini, R. *J. Chem. Phys.* **2006**, *125*, 124508.
(60) Lopez, E. R.; Pensado, A. S.; Comunas, M. J. P.; Padua, A. A. H.; Fernandez, J.; Harris, K. R. *J. Chem. Phys.* **2011**, *134*, 144507.
(61) Habasaki, J.; Casalini, R.; Ngai, K. L. *J. Phys. Chem. B* **2010**, *114*, 3902.